Engineering herpes simplex viruses by infection-transfection methods including recombination site targeting by CRISPR/Cas9 nucleases

Tiffany A. Russell[a], Tijana Stefanovic[a] and David C. Tscharke[a, #]

[a]Research School of Biology, Bldg #134 Linnaeus Way, The Australian National University, Canberra, ACT, 0200, Australia (tiffany.russell@anu.edu.au; tijana.stefanovic@anu.edu.au; david.tscharke@anu.edu.au).

[#]Address for correspondence: David Tscharke, Research School of Biology, Bldg #134 Linnaeus Way, The Australian National University, Canberra ACT 0200, David.Tscharke@anu.edu.au, T: +61 2 6125 3020, F: +61 2 6125 0313

13 **Summary**

14 Herpes simplex viruses (HSV) are frequent human pathogens and the ability to engineer
15 these viruses underpins much research into their biology and pathogenesis. Often the
16 ultimate aim is to produce a virus that has the desired phenotypic change and no additional
17 alterations in characteristics. This requires methods that minimally disrupt the genome and,
18 for insertions of foreign DNA, sites must be found that can be engineered without disrupting
19 HSV gene function or expression. This study advances both of these requirements. Firstly,
20 the use of homologous recombination between the virus genome and plasmids in
21 mammalian cells is a reliable way to engineer HSV such that minimal genome changes are
22 made. This has most frequently been achieved by cotransfection of plasmid and isolated
23 viral genomic DNA, but an alternative is to supply the virus genome by infection in a
24 transfection-infection method. Such approaches can also incorporate CRISPR/Cas9 genome
25 engineering methods. Current descriptions of infection-transfection methods, either with or
26 without the addition of CRISPR/Cas9 targeting, are limited in detail and the extent of
27 optimisation. In this study it was found that transfection efficiency and the length of
28 homologous sequences improve the efficiency of recombination in these methods, but the
29 targeting of the locus to be engineered by CRISPR/Cas9 nucleases has an overriding
30 positive impact. Secondly, the intergenic space between U_L26 and U_L27 was reexamined as
31 a site for the addition of foreign DNA and a position identified that allows insertions without
32 compromising HSV growth *in vitro* or *in vivo.*

33 **Keywords**

34 Herpes simplex virus, genome engineering, recombinant virus, CRISPR, Cas9

1. Introduction

Herpes simplex virus (HSV) types 1 and 2 are highly prevalent human pathogens, with HSV-1 infecting approximately 60% of people worldwide (Cunningham et al., 2006; Bradley et al., 2014). HSV is also extensively studied as the prototypical alphaherpesvirus due to the relative ease with which it can be grown and the wide variety of *in vitro* and *in vivo* models available (Simmons Nash, 1984; Sawtell Thompson, 1992; Shimeld et al., 1996; Leland Ginocchio, 2007; Hogk et al., 2013). Recombinant HSV expressing foreign genes have proven invaluable for studying viral pathogenesis and growth, as well as for screening for potential antiviral agents (Tanaka et al., 2004; Balliet et al., 2007; Ramachandran et al., 2008; Ding et al., 2012). Further, HSV has shown some promise as a recombinant vaccine vector, especially against cancer (Markert et al., 2000; Rampling et al., 2000; Goins et al., 2008). Ideally methods for making recombinant HSV should a) leave minimal changes other than those desired in the genome and b) where foreign genes are added, these should be inserted at sites that do not impact the growth and pathogenesis of the virus.

The original method for making such viruses relies upon homologous recombination between a transfer plasmid that has copies of the viral sequences flanking the desired insertion site and the virus genome in cultured mammalian cells. The relatively low rate at which this occurs means that efficient methods are required to select or screen the few recombinant viruses that are produced (Tanaka et al., 2004; Ramachandran et al., 2008). More recently, recombineering of HSV genomes propagated as Bacterial Artificial Chromosomes, or BACs, has been used. However, viruses recovered from these usually contain residual BAC sequences and/or are attenuated *in vivo* due to other unwanted changes (Horsburgh et al., 1999; Tanaka et al., 2003; Gierasch et al., 2006). Therefore, the original methods remain essential tools that continue to be used.

In non-BAC homologous recombination-based methods, cotransfection of viral and transfer plasmid DNA is the most common way of generating recombinant HSV. While detailed

reports in the literature are sparce, anecdotally this relies heavily on obtaining very high quality HSV genomic DNA. A simpler alternative is to provide the HSV genome by infection of cells transfected with a transfer plasmid (transfection/infection) and at least one report of the use of such as method can be found, but few details were included (Orr et al., 2005). Transfection/infection is also a common way to engineer poxviruses, which have large dsDNA genomes that unlike HSV are non-infectious (Mackett et al., 1984; Wong et al., 2011). In addition, such methods can be combined with CRISPR/Cas9 genome editing tools (Bi et al., 2014; Suenaga et al., 2014). However, thus far the improvement in recombination frequency associated with the application of CRISPR/Cas9 targeting has not been made against optimised transfection/infection methods.

A variety of different locations have been identified in the HSV-1 genome which allow the insertion of foreign DNA with minimal disruption of genes. These include intergenic regions between U_L3 and U_L4, U_L50 and U_L51 and U_S1 and U_S2, but only the first of these has been well characterized (Tanaka et al., 2004; Morimoto et al., 2009). In each case, the genes either side of the insertion site are convergently transcribed and each has its own polyA signal between which there is enough sequence for an insertion to be made without disrupting either transcription unit. Most other common sites of insertion, such as the U_S5/U_S6 location and U_L23 (thymidine kinase) lead to disruption of some ORFs, generally leading to attenuation *in vivo* (Rinaldi et al., 1999; Proenca et al., 2008). The space between U_L26 (glycoprotein B, gB) and U_L27 genes has the ideal structure described above, but previous attempts to use this insertion site have led to some loss of virulence (Halford et al., 2004; Orr et al., 2005). It remains possible that this site can accept insertions without compromising virulence if these are targeted to ensure there is no disruption of the transcription units, including polyA sites.

The aims of this study were to explore transfection-infections approaches for generating recombinant HSV, including CRISPR/Cas9 targeting and to identify a precise position between U_L26 and U_L27 where foreign genes can be inserted without loss of virulence.

2. Materials and Methods

2.1. Viruses and cell lines

The unmodified HSV-1 strain KOS was provided by Francis Carbone (University of Melbourne, Australia). HSV-1 pCmC contains the fluorescent reporter mCherry under the control of the cytomegalovirus immediate early (CMV IE) promoter located in the intergenic region between U_L3 and U_L4 of HSV-1 KOS (HSV-1 KOS 11649). This virus was constructed by standard homologous recombination based methods following four rounds of plaque purification.

All viruses were grown and titrated on Vero cells (ATCC CCL-81). The immortalized Vero cell line was maintained in Minimal Essential Medium (MEM; Gibco/Life Technologies, Carlsbad, USA) supplemented with 2 or 10% heat-inactivated fetal calf serum, 5 mM 4-(2-hydroxyethyl)-1-piperazineethanesulfonic acid, 4 mM L-glutamine and 50 mM 2-mercaptoethanol. All transfections were carried out on 293A cells with Lipofectamine 2000 (Life Technologies, Carlsbad, USA).

2.2. Plasmid construction

All sequence references below are to the HSV-1 genome, accession JQ673480. To construct the generic transfer vector pT $U_L3/4$, the U_L3/U_L4 region (HSV-1 10534-12682) was cloned into pTracer CMV/bsd (Life Technologies, Carlsbad, USA) by In-Fusion cloning (Clontech Laboratories, Mountain View, USA). These HSV-1 sequences were generated in two polymerase chain reactions (PCR) to enable the addition of *EcoRV*, *PstI* and *SpeI* sites between the polyA signals of U_L3 and U_L4 (HSV-1 11649) by the use of extended primers to make pT $U_L3/4$.

The cytomegalovirus immediate early (CMV IE) promoter and bovine growth hormone (BGH) poly A termination sequence were amplified from pTracer CMV/bsd and the eGFP Cre

cassette was amplified from pIGCN21 (Lee et al., 2001). These fragments were then cloned into the *SpeI* site of pT $U_L3/4$ by In-Fusion cloning to construct pT pC_eGC (Fig 1A).

To construct plasmids with different lengths of homology sequence, sequences flanking the intergenic U_L3/U_L4 region were amplified and cloned into the pCR bluntII vector (Life Technologies, Carlsbad, USA). Four plasmids were made in this way, namely pU3.0.5kbF (HSV-1 11200-12179), pU3.1kbF (HSV-1 10700-12722), pU3.2kbF (HSV-1 9803-13698) and pU3.3kbF (HSV-1 8689-14663), such that a MCS containing *KpnI* and *NotI* sites are inserted in the middle of a fragment of the U_L3/U_L4 intergenic region (HSV-1 11649). The following three synthetically constructed elements were inserted into the MCS of each of these plasmids (Genscript, Piscataway, USA): A) The ICP47 promoter lacking the origin of replication (OriS) sequence (Summers Leib, 2002). The sequence encoding the OriS was removed as it has been shown that this plays no role in regulating the transcription of ICP47 (Summers Leib, 2002). B) A Venus reporter gene containing a SV40 nuclear localization sequence. C) A BGH polyA terminator sequence. The resulting plasmids were named pU3.0.5kbF-Venus, pU3.1kbF-Venus, pU3.2kbF-Venus and pU3.3kbF-Venus (Fig 2A).

To construct pU26/7, the U_L26/U_L27 region (HSV-1 51431-54154) with *EcoRV*, *NotI* and *SpeI* sites added between the two polyA signals (at HSV-1 52809) was inserted into pUC19 (Clontech Laboratories, Mountain View, USA) to make pU26/7. Into the *Not*I site of this generic vector was inserted the ICP47 promoter (described above) upstream of a Tdtomato gene with a BGH polyA termination sequence (from pCIGH3) to make pU26/7 pICP47/TdTom (Fig 3C).

The plasmid pX330 (Addgene plasmid 42230) has been previously (Cong et al., 2013). The plasmid pX330-mC was constructed by annealing two complimentary oligodeoxynucleotides (CACCGGATAACATGGCCATCATCA and AAACTGATGATGGCCATGTTATCC) and ligating the resulting dsDNA fragment into the BbsI site of pX330.

2.3. Generation of recombinant HSV-1 by transfection/infection

Recombinant HSV-1 were produced by transfection of 293A cells with the required amount of plasmid DNA. After 5 hours incubation (37°C, 5% CO_2), cells were infected with HSV-1 KOS at an appropriate MOI. All cell-associated and supernatant virus was harvested from the transfection with the aid of a cell lifter. This was then subjected to three cycles of freezing and thawing to lyse the cells and release the virus. The virus was then serially diluted and used to infect fresh cultures of Vero cells overlaid with phenol red-free semisolid MEM-2 with 0.4% (w/v) carboxy-methyl cellulose (M2-CMC). This allowed the development of individual plaques after 48 hours which were then able to be identified and selected by fluorescence microscopy. Multiple rounds of plaque purification were carried out as appropriate. PCR screening and sequencing was used to confirm the correct modification occurred and to identify plaque isolates free of parental virus where appropriate. Two independent recombinant viruses were isolated from parallel transfection/infection experiments.

2.4. Replication *in vitro*

Confluent Vero cell monolayers in six well plates were infected with 1×10^4 PFU (MOI 0.01) virus in 1 mL M0. After 1 h at 37°C, virus inocula were removed, the cell monolayer was washed once and 2 mL fresh M2 added. The first samples (zero hour) were harvested immediately after the addition of fresh media and virus from further wells was collected at the times indicated. To harvest virus, cells were scraped into the media so that both were collected in a single sample. These were subjected to three freeze/thaw cycles and virus titres in each determined by plaque assay on Vero cells.

2.5. Measurement of Plaque Size

Confluent Vero cell monolayers in six well plates were infected with 50 PFU virus. After incubation for 90 min at 37°C, 5% CO_2, the inoculum was replaced with M2-CMC. 48 hours later, cells were crystal violet stained and 30 representative photographs per virus were

taken at 100x magnification using an Olympus CKX41 microscope and DP20 camera. Plaque area was calculated using ImageJ (Rasband, 1997-2012).

2.6. Mice and infections

This study was carried out in accordance with the Australian NHMRC guidelines contained within the Australian Code of Practice for the Care and Use of Animals for Scientific Purposes. Female specific pathogen free C57Bl/6 mice greater than 8 weeks of age were obtained from the APF (Canberra, Australia). Mice were housed and experiments carried out according to ethical requirements and under approval of the Animal Ethics Committee of the Australian National University (Protocol Number: A2011.001).

To assess the virulence of HSV, a mouse flank infection model was used where virus was introduced onto the flanks of shaved mice using a tattoo machine (Figure S1). This is a variation of the flank scarification or abrasion technique sometimes referred to as the zosteriform model (Blyth et al., 1984; Van Lint et al., 2004). The advantage of tattooing over scarification is that the skin remains unbroken by the inoculation, so on the first day after infection there is no sign of damage to the skin allowing the development of the primary lesion to be clearly observed from two days later (Fig S1A). After five days, secondary (or zosteriform) spread is seen, usually peaking on day seven and typically all lesions resolve by 14 days after infection (Fig. S1B).

Female C57Bl/6 mice eight weeks of age or greater were used. Mice were anaesthetized by i.p. injection of avertin (1,1,1 Tribromoethanol in 2-methyl-2-butanol) given at 250 mg/kg and kept warm when not being handled using an infrared lamp. The left flank of each mouse was clipped and depilated with Veet cream (Reckitt Benckiser; Sydney, Australia). For tattooing, a 10 round shader needle (a cluster containing 10 needles in a round pattern) was mounted on a Swiss rotary tattoo machine (Pullman Tools; Widnau, Switzerland) and charged with virus by dipping for 10 seconds in a suspension containing 1×10^8 PFU/mL HSV. The site for infection was determined by identifying the tip of the spleen (seen through the skin) and a

5 × 5 mm area was tattooed for 10 seconds with gentle pressure and even coverage of the area. Mice were monitored daily following infection for lesion development. Where mice have been weighed they generally lose around 5% of body weight in the days after the infection procedure and then recover; there is no evidence of generalized illness as a result of lesion formation.

2.7. Titration of virus from skin and dorsal root ganglia (DRG)

A 1 cm^2 portion of skin located over the inoculation site and the 10 DRG on the ipsilateral side corresponding to spinal levels L1 – T5 were collected from each mouse 5 days after infection. Samples were homogenized in M2, subjected to three cycles of freeze/thawing and infectious virus quantified by plaque assay on Vero cells.

2.8. Statistical analysis

Statistical comparisons were performed using an unpaired t-test with Welch's correction with the aid of Prism software (version 5.01; GraphPad, La Jolla, USA).

3. Results

3.1. Transfection/infection methods for generating recombinant HSV-1

To establish the transfection/infection method a recombinant HSV was designed that would express a fusion protein of enhanced green fluorescent protein and Cre recombinase (eGFP/Cre) using the cytomegalovirus immediate early (CMV IE) promoter from the intergenic space between HSV U_L3 and U_L4 genes. A fluorescent reporter was chosen to enable the easy identification of recombinant viruses and the U_L3/U_L4 intergenic region was selected because insertions at this site do not compromise growth or virulence (Tanaka et al., 2004; Morimoto et al., 2009). The point of insertion was between the two native polyA sequences which are necessary for proper termination of U_L3, U_L4 and U_L5 transcription

(Morimoto et al., 2009). The plasmid used (pT pC_eGC) and the eGFP/Cre expression cassette are shown in Figure 1A.

Three parameters associated with infection/transfection were tested to determine which were important determinants of the frequency of recombinant virus generation: 1) the amount of virus, or multiplicity of infection (MOI); 2) the efficiency of transfection; 3) the length of flanking region sequence.

To determine if the amount of virus used to infect the cells influenced the frequency of recombination, 293A cells were transfected with linearized pT pC_eGC DNA five hours prior to infection with HSV-1 strain KOS at MOIs of 0.01, 0.001 or 0.0001. Virus was harvested after three days and serial dilutions used to infect new cultures. This allowed quantification of $eGFP^+$ and $eGFP^-$ progeny. As expected, as MOI increased, total virus yields were correspondingly higher but proportions of $eGFP^+$ and $eGFP^-$ plaques remained similar (Fig 1B).

Next, to examine transfection efficiency, varied amounts of linearized or circular plasmids were transfected into 293A cells to achieve differing transfection efficiencies as measured by flow cytometry. These cells were then infected with HSV-1 KOS at an MOI of 0.01 and after three days, virus was harvested. Serial dilutions of this virus were used to infect new cultures and the proportion of total plaques that were $eGFP^+$ was determined (Fig 1C, D). Higher transfection efficiency improved the proportion of $eGFP^+$ plaques in a roughly linear manner and notably, efficiencies below 20% did not reliably produce any recombinants.

The third parameter tested was the length of viral sequences flanking the insertion site used in the transfer plasmid. Plasmids were generated that contained left and right flanks either side of the U_L3/U_L4 intergenic region of approximately 0.5, 1, 2, or 3 kb (Fig 2A). Venus was chosen as a marker so that we could continue to use fluorescence to identify recombinant viruses while widening the range of foreign genes shown to be inserted using the

transfection/infection method. In two independent experiments, these Venus transfer plasmids were transfected into 293A cells with conditions that ensured transfection efficiency was similar (~70 - 80% by flow cytometry, not shown) and then infected with HSV-1 at an MOI of 0.01. As in previous experiments, virus was harvested after 3 days. The proportion of $Venus^+$ plaques of total virus was determined by fluorescence microscopy of cell monolayers infected with serial dilutions of the progeny from these transfection/infections (Fig 2B). In both experiments the frequency of $Venus^+$ plaques was directly proportional to the length of the flanking sequence in the transfer plasmids with the range of efficiency across the plasmids being in the order of 10-fold.

3.2. CRISPR/Cas9 targeting of the recombination site has an overriding influence on recombination frequency of transfection-infection methods

The methods detailed above gave recombination frequencies high enough to allow visual selection of viruses engineered to express a fluorescent marker, but even with the optimizations made thus far it would remain challenging to identify recombinants without this visual aid. The recently developed use of CRISPR/Cas9 genome engineering approaches offers an avenue to improve the efficiency of homologous recombination in a variety of settings (Cong et al., 2013). These methods use an RNA guided nuclease (Cas9) to cleave dsDNA at a desired position and these double-stranded breaks can be repaired either by non-homologous end joining or, if a suitable template is available, homologous recombination (Cong et al., 2013). There have been two reported applications that used CRISPR/Cas9 to aid the generation of recombinant HSV-1, but little optimisation was reported (Bi et al., 2014; Suenaga et al., 2014).

First, a preliminary experiment was done that found co-transfection of the transfer plasmid with a CRISPR/Cas9 construct designed to cleave the HSV genome at the site of recombination greatly improved the frequency of recombinant HSV that can be obtained by transfection-infection (not shown). Next, the impact of two parameters associated with the

incorporation of CRISPR/Cas9 plasmids into the strategy were examined 1) the length of the flanking region sequence in the transfer plasmid and 2) the ratio of the CRISPR-Cas9 targeting plasmid to the repair plasmid used.

To test the first of these, Venus transfer plasmids (as described in Fig. 2A) were transfected into 293A cells such that transfection efficiency was similar along with either pX330-mC (that will cleave mCherry coding sequence) or pX330 (a control with no targeting sequence) in a 1:1 ratio. Five hours later, these cells were infected with HSV-1 pCmC at an MOI of 0.01. Virus was harvested after 3 days and used to infect new cultures and the numbers of $Venus^+$, $mCherry^+$ and non-fluorescent plaques were determined by microscopy (Fig 3A). The use of the mCherry-targeting pX330-mC had a dramatic effect, improving the frequency of $Venus^+$ plaques by >100-fold and up to almost a third of all plaques in one case. In the presence of the mCherry targeting plasmid, increasing the length of flanking region sequence made only a marginal difference in two independent experiments.

In the previous experiment a substantial proportion of plaques were non-fluorescent, indicating that the genome had been cleaved by CRISPR-Cas9, but was repaired without recombination with the repair plasmid. Therefore, it was reasoned that altering the ratio of the repair plasmid DNA to pX330-mC may increase the frequency of the desired recombinant virus. To test this 293A cells were transfected with 2 µg of the repair plasmid pU3.1kbF-Venus and various amounts of pX330 or pX330-mC to generate molar ratios of 4:1, 2:1, 1:1 or 1:2, and then infected with HSV-1 pCmC at an MOI of 0.01. Virus was harvested after 3 days and the proportion of $Venus^+$, $mCherry^+$ and fluorescence negative plaques determined by microscopy of cell monolayers infected with serial dilutions of the progeny from these transfection/infections (Fig. 3B). This experiment further confirmed the large improvement in efficiency associated with CRISPR/Cas9 targeting. Altering the ratio of the CRISPR-Cas9 plasmid to the repair plasmid only had a modest impact on the frequency of fluorescent virus generated and this was repeated in a second experiment.

3.3. Foreign genes can be inserted between U_L26 and U_L27 of HSV-1 without loss of virulence

To develop the U_L26-U_L27 intergenic region as a site that can accept foreign genes available annotations of this region with predicted transcription termination sites were inspected. An insertion position between base pairs 52809 and 52810 (based on the KOS sequence, accession JQ673480) was chosen being roughly equidistant between the full polyA sites for these transcription units (Fig 3A, B). This information was used to design transfer plasmid pUC26/7 into which a cassette containing the ICP47 promoter, TdTomato coding sequence and a BGH polyA signal was inserted (Fig 4C). The transfection/infection method detailed above, without the aid of CRISPR/Cas9 was used to generate recombinant virus. Two TdTomato$^+$ plaques were selected from the progeny of two independent transfection/infections and pure stocks of both were obtained after three rounds of plaque purification. One of these (named HSV-1 pICP47/TdTom) was chosen for further examination and restriction digests of the genome and PCR and DNA sequencing done to confirm its integrity (not shown). This virus was found to have identical replication kinetics compared with the parent KOS in Vero cells (Fig 3D). In addition, HSV-1 pICP47/TdTom also exhibited a normal plaque phenotype (by microscopy) and size (Fig 3E&7; ImageJ, Rasband, 1997-2012). Finally this virus was compared with its parent HSV-1 KOS in a flank model of infection in which virus is introduced by tattoo (Supplemental Fig. S1). The virulence of the HSV-1 pICP47/TdTom was similar to KOS based on observation of lesions (not shown) and virus loads in DRG and skin (Fig 3G).

4. Discussion

This study shows that transfection/infection methods are sufficiently efficient to reliably generate recombinant HSVs where a strong marker for screening, for example a fluorescent protein, is available. In total this method has been used to generate ten viruses using either

317 the U_L3-U_L4 or the U_L26-U_L27 sites and expressing a range of fluorescent proteins under
318 the control of several promoters, some of which are published elsewhere (Mackay et al.,
319 2013; Macleod et al., 2014). For this approach, transfection efficiency is of key importance,
320 with efficiencies of >20% being required and higher efficiencies being preferable. In addition,
321 increasing flank sequence lengths in transfer plasmids improved the frequency of
322 recombination in a roughly linear manner. However, these improvements need to be
323 weighed against the lower transfection efficiencies typically achieved with larger plasmids.
324 Despite influencing efficiency by up to 10-fold, none of these optimizations improved
325 efficiency to the point that recombinant viruses could be identified by PCR screening in the
326 absence of an additional selectable marker to enrich the desired viruses. By contrast the use
327 of CRISPR/Cas9 targeting dramatically improved the frequency of initial recombination. The
328 data above show in some cases a third of all progeny are recombinant using this method.
329 Several more viruses have been generated using this method and frequencies have been as
330 high as 70% and viruses with small deletions and no markers have been made (not shown).
331 Further, the importance of using transfer plasmids with long homology sequences flanking
332 the insertion site is greatly reduced when CRISPR/Cas9 is used. The availability of
333 CRISPR/Cas9 plasmids in repositories and the relative insensitivity of the methods to
334 changes in protocol such as ratio of plasmid suggest that adoption of this technology will
335 greatly expand the accessibility of recombinant virus generation for HSV-1.
336
337 In terms of developing insertion sites, a position between the polyA signals associated with
338 the U_L26 and U_L27 transcription units was chosen and a plasmid designed so that no HSV
339 sequence was deleted. It remains unclear why previous attempts to use this region to add
340 genes as led to attenuation (Halford et al., 2004; Orr et al., 2005). However, in the best
341 described case, the insertion disrupted the native polyA signal of U_L26, which was then
342 replaced with one from SV40 (Orr et al., 2005). This suggests that all elements associated
343 with transcription in this region cannot be easily replaced or predicted. The design detailed in
344 Figure 4 avoids these problems as shown by the generation of HSV-1 pICP47/TdTom, which

had wild type virulence. This establishes a new site that can be used for future recombinant viruses.

Acknowledgements

We wish to thank RSB animal services for husbandry of mice. We thank Francis Carbone (University of Melbourne) for HSV-1 KOS, the National Cancer Institute (NIH) Biological Resources Branch for pIGCN21 and Andrew Lew (Water and Eliza Hall Institute, Melbourne) for pCIGH3. This work was funded by NHMRC Project grant APP1005846 and ARC Future Fellowship FT110100310.

References

Balliet, J.W., Kushnir, A.S., Schaffer, P.A., 2007. Construction and characterization of a herpes simplex virus type I recombinant expressing green fluorescent protein: Acute phase replication and reactivation in mice. Virol. 361, 372-383.

Bi, Y., Sun, L., Gao, D., Ding, C., Li, Z., Li, Y., Cun, W., Li, Q., 2014. High-efficiency targeted editing of large viral genomes by RNA-guided nucleases. PLoS Pathog. 10, e1004090.

Blyth, W.A., Harbour, D.A., Hill, T.J., 1984. Pathogenesis of zosteriform spread of Herpes Simplex virus in the mouse. J. Gen. Virol. 65, 1477-1486.

Bradley, H., Markowitz, L.E., Gibson, T., McQuillan, G.M., 2014. Seroprevalence of Herpes Simplex Virus Types 1 and 2—United States, 1999–2010. J. Infect. Dis. 209, 325-333.

Cong, L., Ran, F.A., Cox, D., Lin, S., Barretto, R., Habib, N., Hsu, P.D., Wu, X., Jiang, W., Marraffini, L.A., Zhang, F., 2013. Multiplex genome engineering using CRISPR/Cas systems. Science 339, 819-823.

Cunningham, A.L., Taylor, R., Taylor, J., Marks, C., Shaw, J., Mindel, A., 2006. Prevalence of infection with herpes simplex virus types 1 and 2 in Australia: A nationwide population based survey. Sex Transm. Infect. 82, 164-168.

Ding, X., Sanchez, D.J., Shahangian, A., Al-Shyoukh, I., Cheng, G., Ho, C.M., 2012. Cascade search for HSV-1 combinatorial drugs with high antiviral efficacy and low toxicity. Int. J. Nanomed. 7, 2281-92.

375 Gierasch, W.W., Zimmerman, D.L., Ward, S.L., VanHeyningen, T.K., Romine, J.D., Leib,
376 D.A., 2006. Construction and characterization of bacterial artificial chromosomes
377 containing HSV-1 strains 17 and KOS. J. Virol. Met. 135, 197-206.
378 Goins, W.F., Krisky, D.M., Wechuck, J.B., Huang, S., Glorioso, J.C. 2008. Construction and
379 production of recombinant herpes simplex virus vectors, Methods Mol. Biol., Vol. 433,
380 pp. 97-113.
381 Halford, W.P., Balliet, J.W., Gebhardt, B.M., 2004. Re-evaluating natural resistance to
382 herpes simplex virus type 1. J. Virol. 78, 10086-10095.
383 Hogk, I., Kaufmann, M., Finkelmeier, D., Rupp, S., Burger-Kentischer, A., 2013. An in vitro
384 HSV-1 reactivation model containing quiescently infected PC12 cells. Biores Open
385 Access 2, 250-7.
386 Horsburgh, B.C., Hubinette, M.M., Qiang, D., MacDonald, M.L., Tufaro, F., 1999. Allele
387 replacement: an application that permits rapid manipulation of herpes simplex virus
388 type 1 genomes. Gene Ther. 6, 922-30.
389 Lee, E.C., Yu, D., Martinez de Velasco, J., Tessarollo, L., Swing, D.A., Court, D.L., Jenkins,
390 N.A., Copeland, N.G., 2001. A highly efficient Escherichia coli-based chromosome
391 engineering system adapted for recombinogenic targeting and subcloning of BAC
392 DNA. Genomics 73, 56-65.
393 Leland, D.S., Ginocchio, C.C., 2007. Role of cell culture for virus detection in the age of
394 technology. Clin. Microbiol. Rev. 20, 49-78.
395 Mackay, L.K., Rahimpour, A., Ma, J.Z., Collins, N., Stock, A.T., Hafon, M.-L., Vega-Ramos,
396 J., Lauzurica, P., Mueller, S.N., Stefanovic, T., Tscharke, D.C., Heath, W.R., Inouye,
397 M., Carbone, F.R., Gebhardt, T., 2013. The developmental pathway for $CD103^{+}CD8^{+}$
398 tissue-resident memory T cells of skin. Nature Immunol. 14, 1294-1301.
399 Mackett, M., Smith, G.L., Moss, B., 1984. General method for production and selection of
400 infectious vaccinia virus recombinants expressing foreign genes. J. Virol. 49, 857-64.
401 Macleod, B.L., Bedoui, S., Hor, J.L., Mueller, S.N., Russell, T.A., Hollett, N.A., Heath, W.R.,
402 Tscharke, D.C., Brooks, A.G., Gebhardt, T., 2014. Distinct APC subtypes drive
403 spatially segregated $CD4^{+}$ and $CD8^{+}$ T-cell effector activity during skin infection with
404 HSV-1. PLoS Pathog. 10, e1004303.
405 Markert, J.M., Medlock, M.D., Rabkin, S.D., Gillespie, G.Y., Todo, T., Hunter, W.D., Palmer,
406 C.A., Feigenbaum, F., Tornatore, C., Tufaro, F., Martuza, R.L., 2000. Conditionally
407 replicating herpes simplex virus mutant, G207 for the treatment of malignant glioma:
408 results of a phase I trial. Gene Ther. 7, 867-74.
409 Morimoto, T., Arii, J., Akashi, H., Kawaguchi, Y., 2009. Identification of multiple sites suitable
410 for insertion of foreign genes in herpes simplex virus genomes. Microbiol. Immunol.
411 53, 155-161.

412 Orr, M.T., Edelmann, K.H., Vieira, J., Corey, L., Raulet, D.H., Wilson, C.B., 2005. Inhibition
413 of MHC class I is a virulence factor in herpes simplex virus infection of mice. PLoS
414 Pathog. 1, 0062-0071.
415 Proenca, J.T., Coleman, H.M., Connor, V., Winton, D.J., Efstathiou, S., 2008. A historical
416 analysis of herpes simplex virus promoter activation in vivo reveals distinct
417 populations of latently infected neurones. J. Gen. Virol. 89, 2965-2974.
418 Ramachandran, S., Knickelbein, J.E., Ferko, C., Hendricks, R.L., Kinchington, P.R., 2008.
419 Development and pathogenic evaluation of recombinant herpes simplex virus type 1
420 expressing two fluorescent reporter genes from different lytic promoters. Virol. 378,
421 254-264.
422 Rampling, R., Cruickshank, G., Papanastassiou, V., Nicoll, J., Hadley, D., Brennan, D.,
423 Petty, R., MacLean, A., Harland, J., McKie, E., Mabbs, R., Brown, M., 2000. Toxicity
424 evaluation of replication-competent herpes simplex virus (ICP 34.5 null mutant 1716)
425 in patients with recurrent malignant glioma. Gene Ther. 7, 859-66.
426 Rasband, W.S. 1997-2012. Image J, U.S. National Institutes of Health, Bethesda, Maryland,
427 USA.
428 Rinaldi, A., Marshall, K.R., Preston, C.M., 1999. A non-cytotoxic herpes simplex virus vector
429 which expresses Cre recombinase directs efficient site specific recombination. Virus
430 Res. 65, 11-20.
431 Sawtell, N.M., Thompson, R.L., 1992. Rapid in vivo reactivation of herpes simplex virus in
432 latently infected murine ganglionic neurons after transient hyperthermia. J. Virol. 66,
433 2150-2156.
434 Shimeld, C., Whiteland, J.L., Williams, N.A., Easty, D.L., Hill, T.J., 1996. Reactivation of
435 herpes simplex virus type 1 in the mouse trigeminal ganglion: An in vivo study of
436 virus antigen and immune cell infiltration. J. Gen. Virol. 77, 2583-2590.
437 Simmons, A., Nash, A.A., 1984. Zosteriform spread of herpes simplex virus as a model of
438 recrudescence and its use to investigate the role of immune cells in prevention of
439 recurrent disease. J. Virol. 52, 816-821.
440 Suenaga, T., Kohyama, M., Hirayasu, K., Arase, H., 2014. Engineering large viral DNA
441 genomes using the CRISPR-Cas9 system. Microbiol. Immunol. 58, 513-522.
442 Summers, B.C., Leib, D.A., 2002. Herpes simplex virus type 1 origins of DNA replication play
443 no role in the regulation of flanking promoters. J. Virol. 76, 7020-7029.
444 Tanaka, M., Kagawa, H., Yamanashi, Y., Sata, T., Kawaguchi, Y., 2003. Construction of an
445 excisable bacterial artificial chromosome containing a full-length infectious clone of
446 herpes simplex virus type 1: viruses reconstituted from the clone exhibit wild-type
447 properties in vitro and in vivo. J. Virol. 77, 1382-1391.

Tanaka, M., Kodaira, H., Nishiyama, Y., Sata, T., Kawaguchi, Y., 2004. Construction of recombinant herpes simplex virus type I expressing green fluorescent protein without loss of any viral genes. Microbes Infect. 6, 485-493.

Van Lint, A., Ayers, M., Brooks, A.G., Coles, R.M., Heath, W.R., Carbone, F.R., 2004. Herpes simplex virus-specific $CD8^+$ T cells can clear established lytic infections from skin and nerves and can partially limit the early spread of virus after cutaneous inoculation. J. Immunol. 172, 392-397.

Wong, Y.C., Lin, L.C.W., Melo-Silva, C.R., Smith, S.A., Tscharke, D.C., 2011. Engineering recombinant poxviruses using a compact GFP-blasticidin resistance fusion gene for selection. J. Virol. Met. 171, 295-298.

Figure Legends

Figure 1. Role of virus multiplicity and transfection efficiency on recombinant HSV generation by transfection/infection. (A) Map of pT pC_eGC indicating the base pair positions of the two flanking regions (in grey), using numbers from HSV-1 KOS (accession JQ673480), other features are as marked. (B) Effect of MOI on virus output of transfection/infections. 293A monolayers were transfected with pT pC_eGC and infected at the MOIs shown 5 hours later. Progeny of these transfection/infections at 72 hrs were used to infect monolayers of Vero cells, and the number of total (open bars) and $eGFP^+$ (black bars) plaques counted. Results are representative of two experiments. (C and D) The effect of transfection efficiency was tested for linearized (C) and intact (D) plasmids. 293A were transfected with pT pC_eGC to achieve a range of efficiencies and infected at an MOI of 0.01 5 hours later. Progeny of these transfection/infections were collected at 72 hours to determine the rate of recombinant virus generation. The proportion of $eGFP^+$ plaques is plotted against the transfection efficiency as determined by flow cytometry.

Figure 2. Influence of flank sequence length on recombinant HSV generation by transfection/infection. (A) Representative map of plasmids with different lengths of U_L3/U_L4 flanking sequences. Four different lengths were used as depicted by the concentric

grey boxes to generate plasmids pU3.0.5kbF (HSV-1 KOS 11200-12179), pU3.1kbF (HSV-1 KOS 10700-12722), pU3.2kbF (HSV-1 KOS 9803-13698) and pU3.3kbF (HSV-1 KOS 8689-14663). Other features are as marked. (B) 293A monolayers were transfected with the each of the plasmids shown in (A) and infected at an MOI of 0.01 5 hours later. Progeny of these transfection/infections was harvested at 72 hours and used to infect monolayers of Vero cells. The percentage of $Venus^+$ plaques of all HSV plaques is shown. Two independent experiments are indicated with markers in grey and black.

Figure 3. Targeting the site of insertion using CRISPR-Cas9 has an overriding effect on recombination frequency. (A) 293A monolayers were cotransfected with 2 µg of one of the plasmids shown in Fig. 2A and either pX330 or pX330-mC in a 1:1 ratio, and infected with HSV-1 pCmC at an MOI of 0.01 5 hours later. Progeny of these transfection/infections was harvested at 72 hours and used to infect monolayers of Vero cells. Pie charts show the percentage of $Venus^+$, $mCherry^+$ and non-fluorescent plaques where mCherry was targeted (with pX330-mC) and boxes below are the approximate percent of $Venus^+$ plaques found when the control (pX330) plasmid was used. (B) 293A monolayers were cotransfected with 2 µg pU3.1kbF-Venus and the appropriate mass of either pX330 or pX330-mC so the ratio of these plasmids was 4:1, 2:1, 1:1 or 1:2, and infected with HSV-1 pCmC at an MOI of 0.01 5 hours later. Progeny of these transfection/infections was harvested at 72 hours and used to infect monolayers of Vero cells. The pie charts and boxes show data as for panel A, nd = not determined. Experiments in A and B were repeated with similar results.

Figure 4. Use of U_L26-U_L27 intergenic region for insertion of foreign DNA into HSV. (A) Schematic representation of the HSV-1 genome with the location of U_L26 and U_L27 indicated. (B) Detail of the insertion of the TdTomato expression cassette in the intergenic space between U_L26 and U_L27. (C) Map of pU26/7 pICP47/TdTom indicating the base pair positions of the U_L26/U_L27 flanking regions (in grey), using numbers from HSV-1 KOS (accession JQ673480), other features are as marked. (D) Multiple step growth analysis (MOI

0.01) in Vero cells comparing parent HSV-1 KOS (shown in black) and HSV-1 pICP47/TdTom (shown in grey). Data are mean±SEM of three replicates. (E and F) Plaques of HSV-1 KOS and pICP47/TdTom on Vero cells under semi-solid media were similar. Morphology (E) is shown by phase contrast microscopy at 100× magnification (scale bar = 150μm) and size (F) was measured for 30 plaques of each virus (mean size indicated by the black bar). (G) Amounts of infectious virus in the skin and innervating DRG of C57Bl/6 mice 5 days after flank infection with HSV-1 KOS (black) and HSV-1 pICP47/TdTom (grey). Circles show results for each mouse (n=4) and bars represent mean±SEM. (*ns* = not significant).

Figure S1. Pathogenesis of HSV in mice following flank infection by tattoo. C57Bl/6 mice were infected with 1×10^8 PFU/mL WT HSV-1 KOS by tattoo. (A) Photographs of a representative mouse were taken at 1, 4, and 7 days after infection. (B) Estimation of total lesion size over time. Circles and bars represent mean±SEM (n=3).

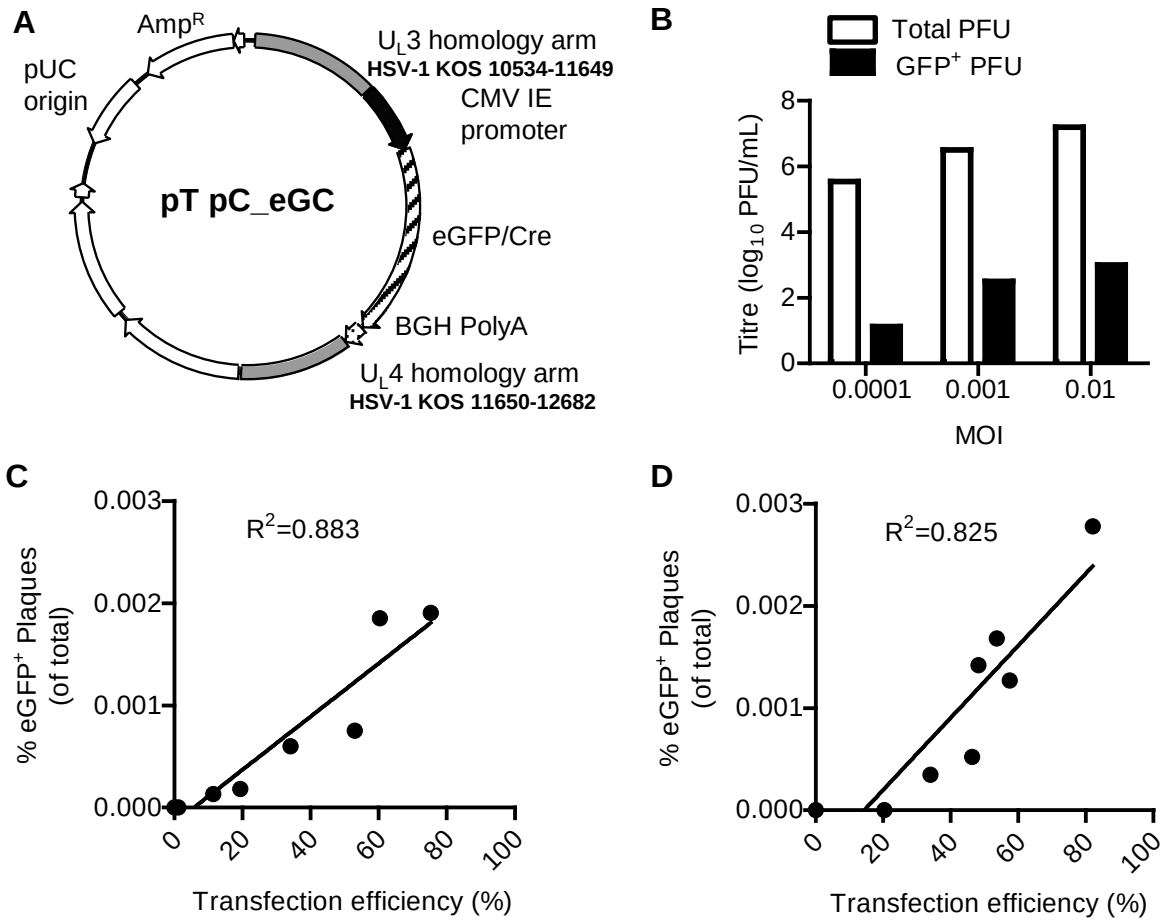

Figure 1. Role of virus multiplicity and transfection efficiency on recombinant HSV generation by transfection/infection. (A) Map of pT pC_eGC indicating the base pair positions of the two flanking regions (in grey), using numbers from HSV-1 KOS (accession JQ673480), other features are as marked. (B) Effect of MOI on virus output of transfection/infections. 293A monolayers were transfected with pT pC_eGC and infected at the MOIs shown 5 hours later. Progeny of these transfection/infections at 72 hrs were used to infect monolayers of Vero cells, and the number of total (open bars) and eGFP$^+$ (black bars) plaques counted. Results are representative of two experiments. (C and D) The effect of transfection efficiency was tested for linearized (C) and intact (D) plasmids. 293A were transfected with pT pC_eGC to achieve a range of efficiencies and infected at an MOI of 0.01 5 hours later. Progeny of these transfection/infections were collected at 72 hours to determine the rate of recombinant virus generation. The proportion of eGFP$^+$ plaques is plotted against the transfection efficiency as determined by flow cytometry.

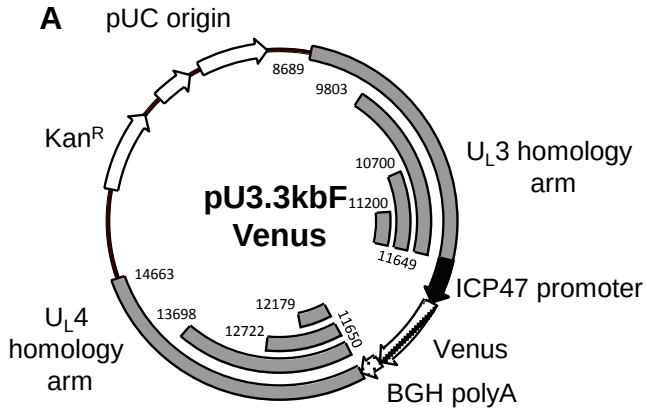

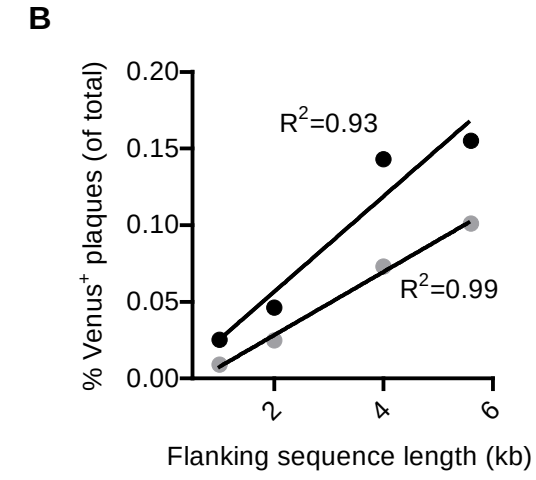

Figure 2. Influence of flank sequence length on recombinant HSV generation by transfection/infection. (A) Representative map of plasmids with different lengths of U_L3/U_L4 flanking sequences. Four different lengths were used as depicted by the concentric grey boxes to generate plasmids pU3.0.5kbF (HSV-1 KOS 11200-12179), pU3.1kbF (HSV-1 KOS 10700-12722), pU3.2kbF (HSV-1 KOS 9803-13698) and pU3.3kbF (HSV-1 KOS 8689-14663). Other features are as marked. (B) 293A monolayers were transfected with the each of the plasmids shown in (A) and infected at an MOI of 0.01 5 hours later. Progeny of these transfection/infections was harvested at 72 hours and used to infect monolayers of Vero cells. The percentage of $Venus^+$ plaques of all HSV plaques is shown. Two independent experiments are indicated with markers in grey and black.

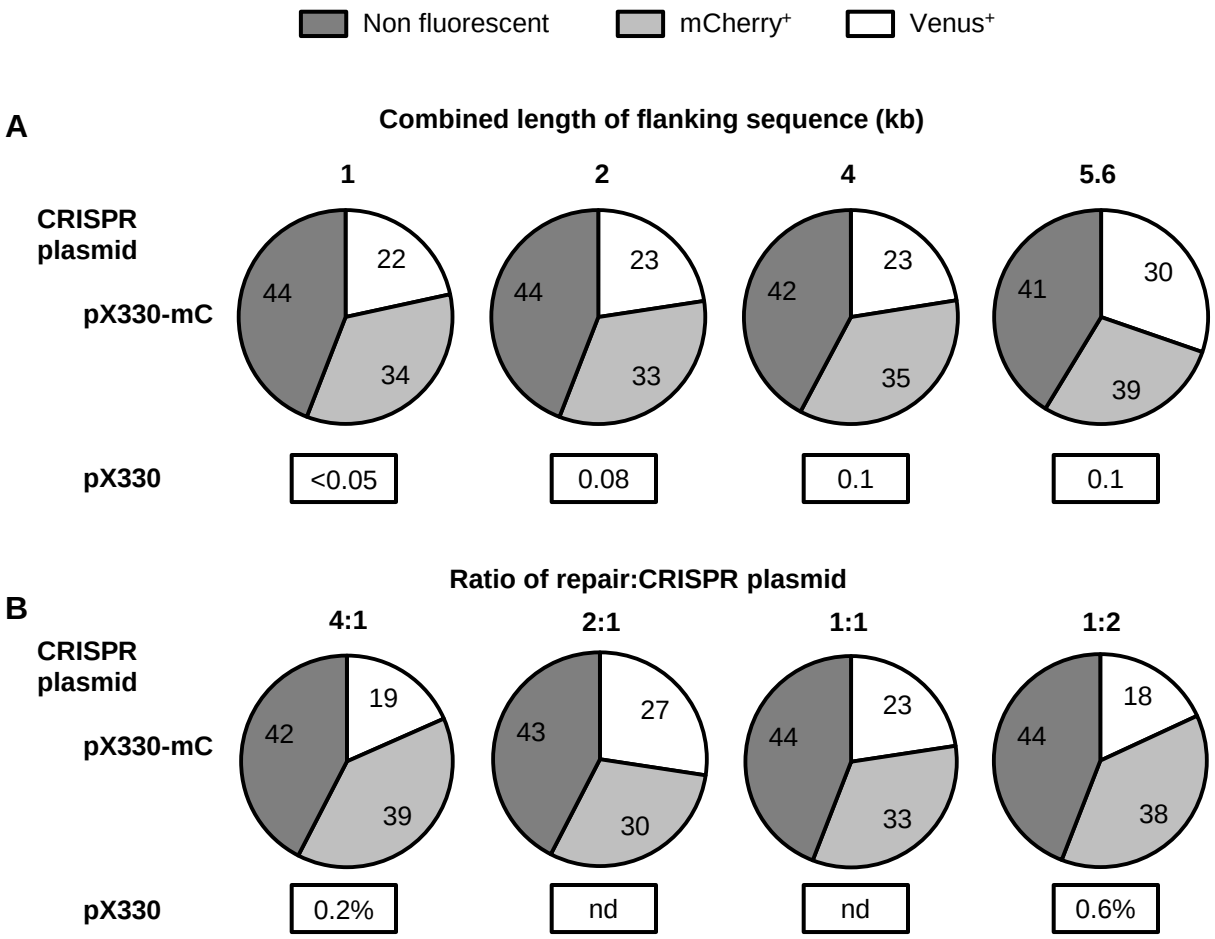

Figure 3. Targeting the site of insertion using CRISPR-Cas9 has an overriding effect on recombination frequency. (A) 293A monolayers were cotransfected with 2 µg of one of the plasmids shown in Fig. 2A and either pX330 or pX330-mC in a 1:1 ratio, and infected with HSV-1 pCmC at an MOI of 0.01 5 hours later. Progeny of these transfection/infections was harvested at 72 hours and used to infect monolayers of Vero cells. Pie charts show the percentage of Venus$^+$, mCherry$^+$ and non-fluorescent plaques where mCherry was targeted (with pX330-mC) and boxes below are the approximate percent of Venus$^+$ plaques found when the control (pX330) plasmid was used. (B) 293A monolayers were cotransfected with 2 µg pU3.1kbF-Venus and the appropriate mass of either pX330 or pX330-mC so the ratio of these plasmids was 4:1, 2:1, 1:1 or 1:2, and infected with HSV-1 pCmC at an MOI of 0.01 5 hours later. Progeny of these transfection/infections was harvested at 72 hours and used to infect monolayers of Vero cells. The pie charts and boxes show data as for panel A, nd = not determined. Experiments in A and B were repeated with similar results.

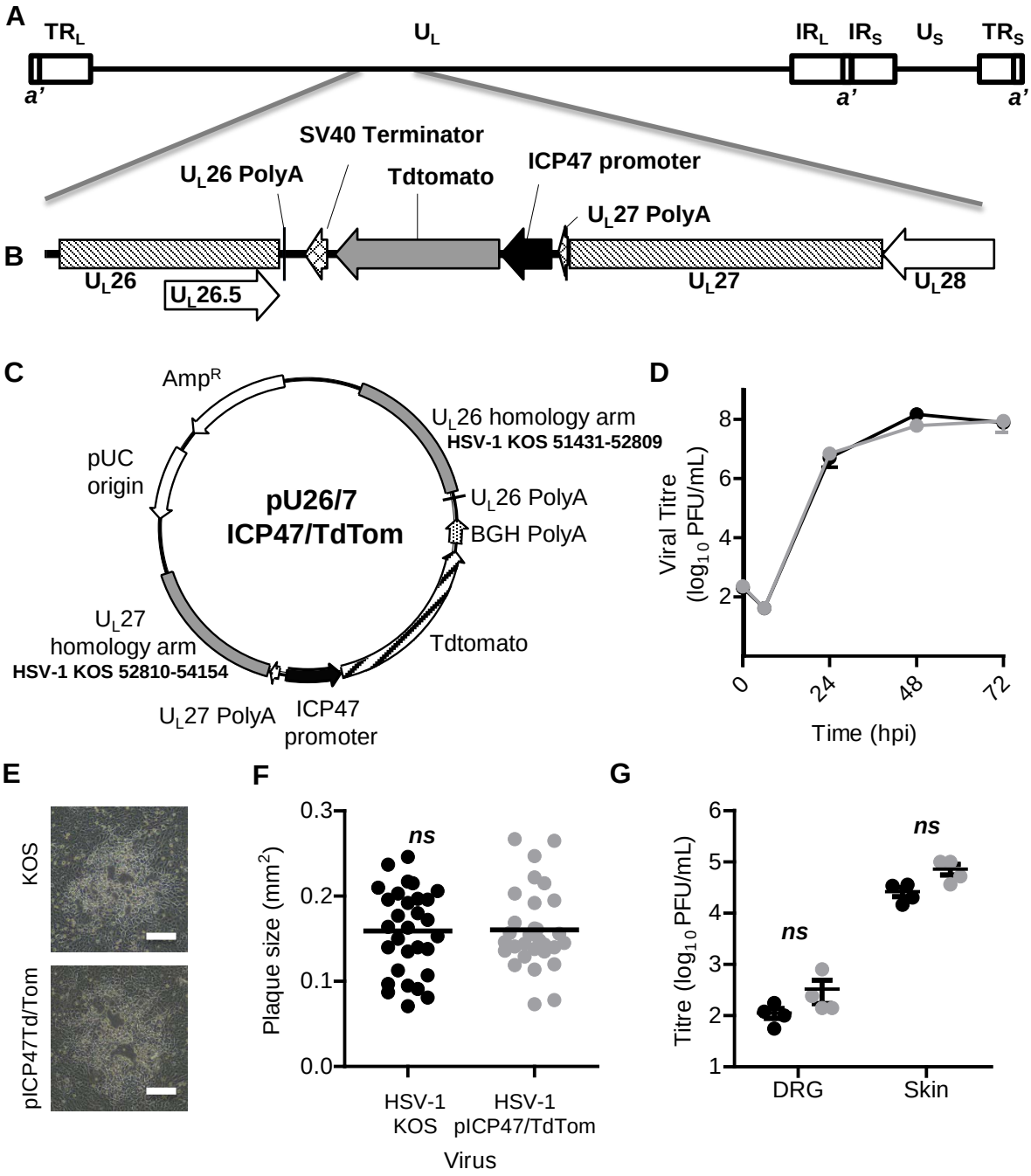

Figure 4. Use of U_L26-U_L27 intergenic region for insertion of foreign DNA into HSV. (A) Schematic representation of the HSV-1 genome with the location of U_L26 and U_L27 indicated. (B) Detail of the insertion of the TdTomato expression cassette in the intergenic space between U_L26 and U_L27. (C) Map of pU26/7 pICP47/TdTom indicating the base pair positions of the U_L26/U_L27 flanking regions (in grey), using numbers from HSV-1 KOS (accession JQ673480), other features are as marked. (D) Multiple step growth analysis (MOI 0.01) in Vero cells comparing parent HSV-1 KOS (shown in black) and HSV-1 pICP47/TdTom (shown in grey). Data are mean±SEM of three replicates. (E and F) Plaques of HSV-1 KOS and pICP47/TdTom on Vero cells under semi-solid media were similar. Morphology (E) is shown by phase contrast microscopy at 100× magnification (scale bar = 150μm) and size (F) was measured for 30 plaques of each virus (mean size indicated by the black bar). (G) Amounts of infectious virus in the skin and innervating DRG of C57Bl/6 mice 5 days after flank infection with HSV-1 KOS (black) and HSV-1 pICP47/TdTom (grey). Circles show results for each mouse (n=4) and bars represent mean±SEM. (*ns* = not significant).

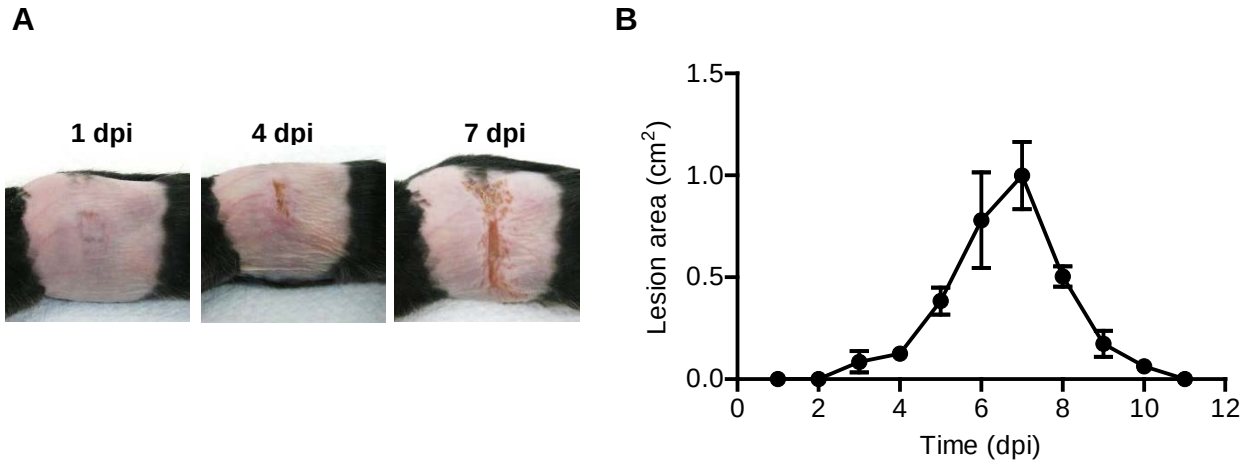

Figure S1. Pathogenesis of HSV in mice following flank infection by tattoo. C57Bl/6 mice were infected with 1 x 10^8 PFU/mL WT HSV-1 KOS by tattoo. (A) Photographs of a representative mouse were taken at 1, 4, and 7 days after infection. (B) Estimation of total lesion size over time. Circles and bars represent mean±SEM (n=3).